Analytic and numerical examples of a leading order imaging subseries

Shaw, S.A.*, Weglein, A.B.*, Foster, D.J.[†], Matson, K.H.[‡], and Keys, R.G.[§]
*University of Houston, [†]ConocoPhillips, [‡]BP, [§]ExxonMobil

This paper was prepared for presentation at the 8th International Congress of The Brazilian Geophysical Society held in Rio de Janeiro, Brazil, 14-18 September 2003.

Abstract

Current methods for depth imaging require an accurate velocity model in order to place reflectors at their correct spatial locations. Techniques to derive the velocity model can fail to provide this information with the necessary degree of accuracy, especially in areas that are geologically complex.

The inverse series, a multi-dimensional direct inversion procedure, has the ability to image reflectors at the correct depth with an inadequate velocity model. In this paper, numerical examples are presented that demonstrate this ability. Convergence of a leading order imaging series is illustrated with 1-D acoustic models when the errors between the reference and actual velocity are large. The effectiveness and robustness of this algorithm warrant its generalization to a multi-dimensional earth, and for more complicated earth model types, both of which are the focus of current work.

Introduction

Our inability to identify and define hydrocarbon targets beneath difficult-to-estimate complex media, e.g., beneath salt, has been and remains a significant impediment to effective exploration and production. Current imaging and inversion methods require an adequate velocity model to produce an adequate image. Frequently, we cannot satisfy that requirement under complex geologic conditions.

The objective of this research is to directly respond to that challenge by developing a fundamentally new capability aimed at accurately imaging and inverting seismic data without knowing or determining the properties of the overburden. In principle, the inverse scattering series has the potential to achieve that objective (Weglein et al., 2000).

This abstract documents part of a long-term research project investigating the use of the inverse scattering series to perform the task of imaging at the correct depth without knowing or determining the actual velocity model. The goal of seismic depth imaging is to produce a spatially accurate map of the reflectivity below the Earth's surface. The inverse series has the potential to achieve this objective without an accurate velocity model. The issues to be resolved are: (1) where within the inverse series does the subseries with that capability reside? (2) what are the limitations on the magnitude and duration of velocity error that it can accommodate? (3) how many terms in the subseries would be required to achieve a specified degree of accuracy? and (4) what are the data requirements and prerequisites to allow the algorithm to be effective?

The inverse series is a multidimensional direct inversion procedure and as such it performs the tasks of removing free surface and internal multiples, locating reflectors at their correct spatial location (imaging), and inverting amplitude information for the actual perturbation (target identification) all in terms of reference, not actual, medium properties. By adopting a strategy of task separation, Weglein et al. (1997) successfully identified two separate subseries of the inverse series that remove free surface multiples and attenuate internal multiples from a multidimensional Earth. The advantages of seeking and isolating subseries that perform single tasks include lower demands on the fidelity of the input data (e.g., band-width, signal-to-noise, etc.), and better convergence properties of the series algorithm. Innanen and Weglein (2003) are investigating the ability of the inverse series to simultaneously perform more than one task (specifically the two tasks of imaging and target identification). In this paper, we present results of a subseries that performs the sole task of imaging in depth.

Terms in the inverse series that are responsible for locating reflectors in their correct spatial location have been identified by Weglein et al. (2002). Early numerical tests of the effectiveness of these terms at imaging primaries for the simplest of 1-D models were encouraging (Shaw, 2001). The identification, development and testing of the imaging subseries have moved to more complicated 1-D layered models that have both significant errors in velocity and duration of that error. In this abstract, we present examples of these 1-D numerical tests and demonstrate convergence, numerically and analytically, of a leading order imaging series (Shaw et al., 2003). The number of terms in the subseries required for accurate imaging depends on the magnitude and duration of the velocity error.

Method

The perturbation, V, is defined as the difference between the actual wave operator, L, and the chosen reference medium's wave operator, L_0. For a one-dimensional constant density acoustic medium with velocity profile $c(z)$ and a homogeneous reference medium with velocity c_0, V has the form

$$V = k_0^2 \alpha \qquad (1)$$

where the index of refraction $\alpha(z)=1-c_0^2/c^2(z)$, $k_0=\omega/c_0$ and ω is the angular temporal frequency. In this context, the inverse series is

$$\alpha = \sum_{n=1}^{\infty} \alpha_n \qquad (2).$$

In the case of a plane wave incident field, the first term in the inverse series is

$$\alpha_1(z) = 4\int_0^z D(z')dz' \qquad (3)$$

where $D(z')$ is the data measured at the surface $z' = 0$. This "trace integration" formula places reflectors at depths z according to

$$z' = c_0 t / 2 \qquad (4)$$

where t is the recorded two-way travel time to the reflector. Equation (3) is the inverse Born approximation, which is the foundation for current depth imaging algorithms. It is linear in the measured values of the scattered field, D. The second term in the inverse series is quadratic in the data. The portion of the second term that is responsible for correcting the depths of the mislocated reflectors in α_1 has been identified by Weglein et al. (2002) as

$$\alpha_2^{LOIS}(z) = -\frac{1}{2}\left(\int_0^z \alpha_1(z')dz'\right)\left[\frac{d}{dz}\alpha_1(z)\right] \qquad (5).$$

Since α_1 is a sum of Heaviside functions, equation (2) produces delta functions at each interface weighted by minus a half times the integral of α_1 down to the output depth, z. The corresponding portion of the third term in the inverse series that is responsible for imaging is

$$\alpha_3^{LOIS}(z) = \frac{1}{8}\left(\int_0^z \alpha_1(z')dz'\right)^2\left[\frac{d^2}{dz^2}\alpha_1(z)\right] \qquad (6)$$

which produces weighted derivatives of delta functions centered at each mislocated interface. The sum of these and higher order imaging terms constitutes the 1-D leading order imaging subseries (LOIS) is (Shaw et al. 2003)

$$\alpha^{LOIS}(z) = \sum_{n=0}^{\infty} \frac{(-1/2)^n}{n!}\left(\int_0^z \alpha_1(z')dz'\right)^n\left[\frac{d^n}{dz^n}\alpha_1(z)\right] \qquad (7)$$

In the next section, we present a numerical example of this algorithm. In essence, it constitutes a Taylor Series for the difference of two Heaviside functions at each mislocated reflector. When the series converges, the reflectors shift from their wrong depths (given by α_1) towards their correct depths (given by α). Fourier transforming equation (7) and recognizing the presence of the series for exp(x) where

$$x(z) = -ik_0\left[1/2\int_0^z \alpha_1(z')dz'\right] \qquad (8)$$

we can write a closed form for the leading order imaging subseries

$$\alpha^{LOIS}(z) = \alpha_1\left(z - 1/2\int_0^z \alpha_1(z')dz'\right) \qquad (9).$$

From equation (9), we see that the leading order imaging series amounts to a stretch of the inverse Born approximation. The stretch itself is proportional to the integral of the Born approximation, and is the leading order approximation to the actual shift. In the frequency domain, this algorithm relates to a phase shift migration where the phase shift is determined directly from a linear inversion of the data.

Since the closed form equation (9) can be derived for any finite $x(z)$, we can conclude that the 1-D leading order imaging series is convergent as long as k_0 and the integral of the perturbation, α, are both finite. Both of these requirements are realizable in practice. Furthermore, we can deduce that the rate of convergence is greater for small values of these two quantities.

Analytic Example

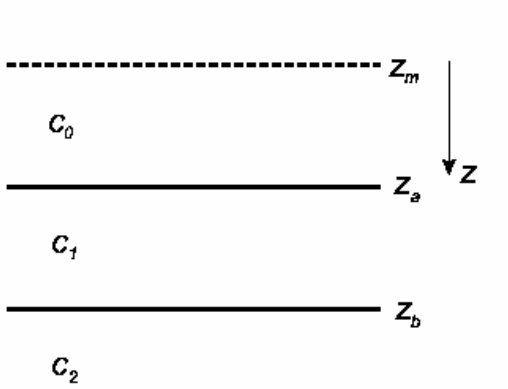

Figure 1. Single layer 1-D Earth model.

Consider the single layer model depicted in Figure 1. We assume that the multiples have been removed from the data. Then, in a normal-incidence plane wave experiment, the recorded wavefield consists of two primary events:

$$D(t) = R_1\delta(t - t_1) + \tilde{R}_2\delta(t - t_2) \qquad (10.)$$

where t_1 and t_2 are the two-way travel times to the first and second reflectors, respectively and

$$R_1 = \frac{c_1 - c_0}{c_1 + c_0}, \quad R_2 = \frac{c_2 - c_1}{c_2 + c_1}$$

$$T_{01} = 1 - R_1, T_{10} = 1 + R_1, \ \tilde{R}_2 = T_{01}R_2T_{10}$$

Then the first term in the imaging series corresponds to a migration-inversion with the constant velocity, c_0

$$\alpha_1(z) = 4R_1\,\mathrm{H}(z - z_a) + \tilde{R}_2\,\mathrm{H}(z - z_{b'}) \quad (11)$$

where H denotes the Heaviside function and

$$z_a = \frac{c_0 t_1}{2}, \quad z_{b'} = \frac{c_0 t_2}{2}$$

$$z_{b'} = z_a + \gamma(z_b - z_a)$$

$$\gamma = \frac{c_0}{c_1}$$

Calculating higher order terms in the leading order imaging subseries yields

$$\alpha_2^{LOIS}(z) = -2R_1(z - z_a)\left[4\tilde{R}_2\delta(z - z_{b'})\right]$$
$$\alpha_3^{LOIS}(z) = 2R_1^{\,2}(z - z_a)^2\left[4\tilde{R}_2\delta'(z - z_{b'})\right]$$
$$\vdots \quad (12).$$

This relates to the series for a shift from the wrong depth $z_{b'}$ to towards the actual depth z_b:

$$4\tilde{R}_2\left[\mathrm{H}(z - z_{b'}) - \mathrm{H}(z - z_b)\right] = 4\tilde{R}_2\left[(z_b - z_{b'})\delta(z - z_{b'}) + \frac{(z_b - z_{b'})^2}{2!}\delta'(z - z_{b'}) + \ldots\right] \quad (13)$$

where the coefficients that are a function of $(z_{b'} - z_b)$ in equation (13) are the leading order (in the data) approximations in equation (12), recognizable from the relationship

$$(z_{b'} - z) = -2(z_{b'} - z_a)\left(R_1 + R_1^{\,2} + \ldots\right).$$

Hence, equation is the leading order imaging subseries. The next section illustrates this algorithm for a band-limited synthetic example.

Numerical Example

Consider the 1-D constant density acoustic model described in Table 1. We use the simple example of a normal incidence plane wave experiment to illustrate the behavior of the leading order imaging subseries.

The left-hand panel of Figure 2 displays the synthetic data for the model described in Table 1 resulting from a 0-125 Hz band-limited incident field. The right-hand panel compares the actual perturbation, α, with the inverse Born approximation, α_1, (the first term in an imaging series). The simplest reference medium, a homogenous whole space (c_0 = 1500 m/s) has been chosen.

Table 1. Depth and velocity pairs that define a 1-D synthetic model.

Layer	Depth to top of layer (m)	Velocity (m/s)
1	0	1500
2	70	1600
3	100	1700
4	120	1550
5	140	1650
6	160	1700

The right-hand panel of Figure 1 illustrates how the first term in the series, which is linear in the data, erroneously locates deep reflectors because the reference velocity does not agree with the actual velocity below the first layer. In addition, the amplitude of α_1 disagrees with that of α. The tasks of correcting the location and amplitude of α_1 reside in the second and higher order terms of the inverse series. The subseries for amplitude inversion (target identification) is being investigated (Zhang and Weglein, 2003).

Figure 2 illustrates the performance of the leading order imaging subseries acting on the input data in Figure 1. The green line is the cumulative sum of *n* terms in the series, where *n* is indicated in the title above each panel. Each new term involves the addition of an $(n - 1)^{th}$ derivative of a band-limited delta function (sinc function) at each mislocated interface. After 27 terms in the imaging series, the second reflector has shifted towards its correct depth, 100 m, and after 40 terms, the next deeper reflector has been located 120 m. After 66 terms, the imaging series has converged at all interfaces and has succeeded in moving the reflectors towards their actual depths. The number of terms required for convergence of the imaging series is proportional to the distance that an interface has to move. This, in turn, depends on the cumulative error in the velocity (difference between the actual and reference) from the surface down to the reflector being imaged.

The right-hand panel in Figure 2 also illustrates the closed form solution (Equation 9) in blue. This solution has the advantage of not suffering from numerical artifacts due to performing so many derivatives.

Conclusions

Analytic and numerical examples of a leading order imaging subseries have been used to demonstrate the intrinsic ability of the inverse series to perform depth imaging in the absence of the actual velocity model. This series converges more rapidly for lower maximum frequencies in the input data, and for smaller cumulative errors between the reference and actual velocity above the reflector. Issues of rate of convergence are mitigated by the compact closed form expression for the imaging

series which also avoids numerical errors that might occur when summing individual terms.

Acknowledgments

The Texas Advanced Research Program (ARP #003652-0624-2001) is acknowledged for partial support of this research. The sponsors of the Mission-Oriented Seismic Research Program are gratefully acknowledged.

References

Innanen, K. and Weglein, A.B. (2003), "Simultaneous imaging and inversion with the inverse scattering series", submitted to 8th International Congress of The Brazilian Geophysical Society.

Shaw, S.A. (2001), "An inverse scattering subseries for predicting the correct spatial location of reflectors: Initial analysis, testing and evaluation", 7th International Congress of The Brazilian Geophysical Society.

Shaw, S.A., Weglein, A.B., Foster, D.J., Matson, K.H., and Keys, R.G. (2003), "Convergence properties of a leading order depth imaging series", submitted to 73rd Annual Meeting of the Society of Exploration Geophysicists, Dallas.

Weglein, A.B., Gasparotto, F.A., Carvalho, P.M., and Stolt, R.H. (1997), "An inverse scattering series method for attenuating multiples in seismic reflection data", Geophysics, **62**, p. 1975-1989.

Weglein, A.B., Matson, K.H., Foster, D.J., Carvalho, P.M.,

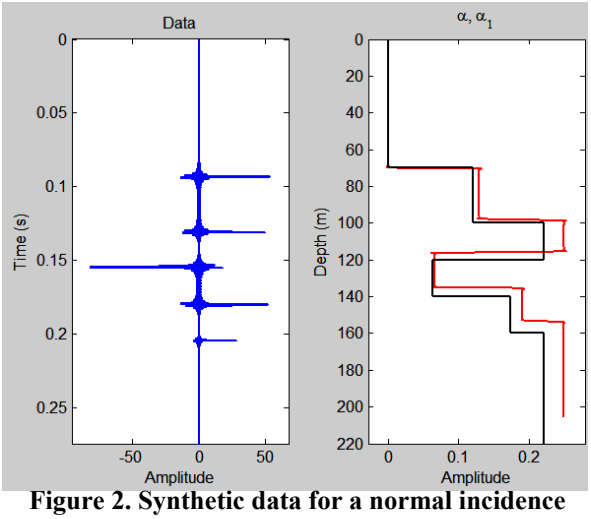

Figure 2. Synthetic data for a normal incidence experiment (left), actual perturbation , α (right, black), and inverse Born approximation, α_1 (right, red).

Corrigan, D., and Shaw, S.A. (2000), "Imaging and inversion at depth without a velocity model", 70th Annual Meeting of the Society of Exploration Geophysicists, Calgary, Canada.

Zhang, H. and Weglein, A.B., (2003), "Target identification using the inverse scattering series; inversion of large-contrast, variable velocity and density acoustic data", M-OSRP, **2**, p. 196, University of Houston.

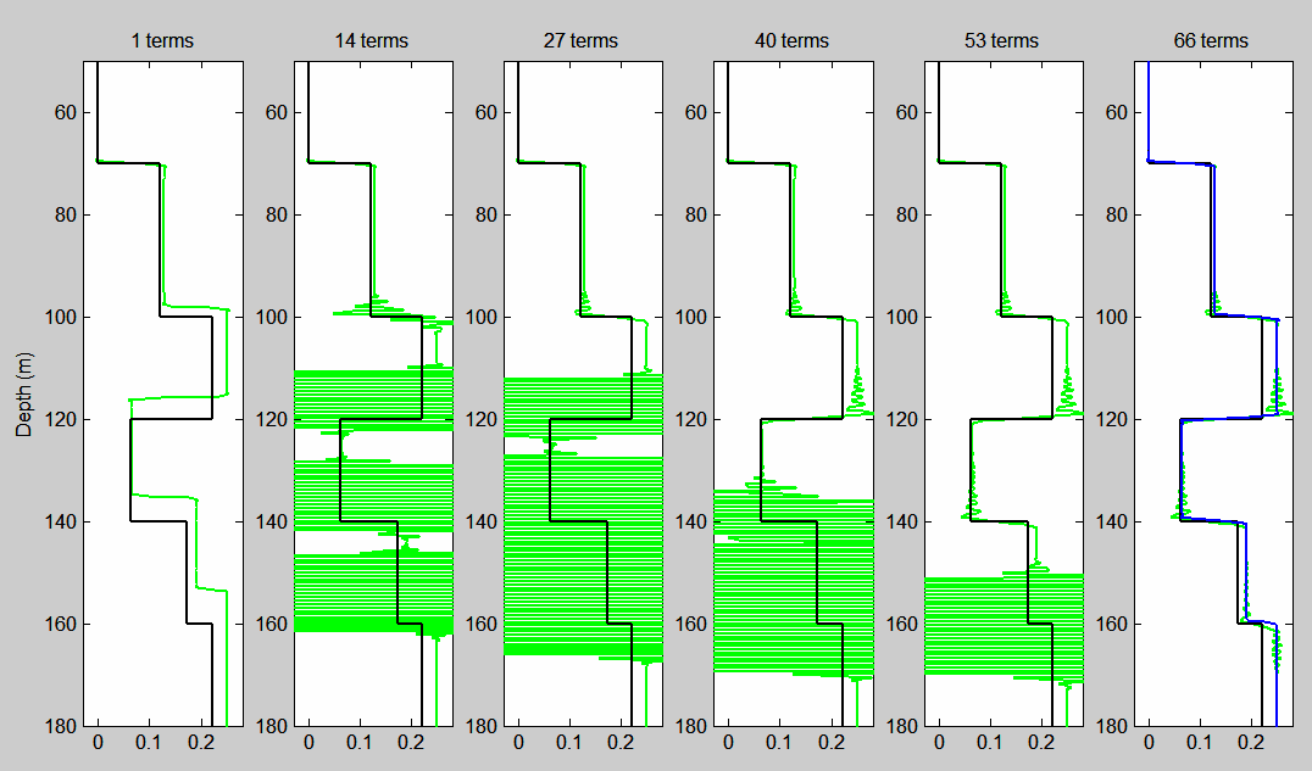

Figure 3. Cumulative sum of terms in the leading order imaging subseries. The actual perturbation α is shown in each panel black, the green trace is the cumulative sum of n terms in the series for α^{LOIS}, where n is given in the title above each panel, and the blue line in the righmost panel is the closed form solution.